2821

A Fast and General Non-Cartesian GRAPPA Reconstruction Method

Tianrui Luo[1], Douglas C. Noll[1], Jeffrey A. Fessler[1], and Jon-Fredrik Nielsen[1]

[1]University of Michigan, Ann Arbor, MI, United States

Synopsis

Iterative parallel imaging reconstruction can be very time-consuming for dynamic imaging applications such as functional MRI. GRAPPA is non-iterative but is generally not well-suited for non-Cartesian acquisitions. In this work, we propose a generalization of GRAPPA applicable to arbitrary non-Cartesian readouts. Our non-Cartesian GRAPPA method works by associating a unique kernel with each unsampled (missing) k-space location, and synthesizing non-Cartesian autocalibration (ACS) data by phase-shifts. This approach requires calibrating a very large number of distinct patterns, for which we propose an efficient NUFFT-like algorithm. With this approach we demonstrate fast reconstruction of 3D stack-of-spirals and stack-of-stars images.

Introduction

GRAPPA[1] is a non-iterative Parallel Imaging (PI) technique that, unlike SENSE, does not require explicit knowledge of coil sensitivity maps (i.e., is auto-calibrating). However, GRAPPA generally assumes Cartesian k-space sampling, and direct application of GRAPPA to arbitrary non-Cartesian trajectories is not possible. Partial workarounds for specific readout trajectories have been proposed, e.g., segmenting spiral trajectories into "wedges" that undergo rectilinear GRAPPA[2], or GROG gridding[3], an approximate interpolation scheme. However, a general GRAPPA reconstruction approach for arbitrary 2D/3D non-Cartesian sampling does not yet exist.

Here we propose a *general* non-Cartesian GRAPPA reconstruction that is not restricted to specific readout trajectories. It works by assigning a unique kernel to each unsampled k-space point. To keep computational costs down, we propose an efficient NUFFT-based algorithm[4]. We apply our method to the reconstruction of 3D stack-of-stars/spirals datasets.

Methods

GRAPPA first identifies all (unique) kernel patterns to be calibrated (Fig.1). Then, for each pattern, all combinations of autocalibration signals (ACS) that match the pattern are obtained. These combinations become the rows of $\tilde{\mathcal{A}} := [\tilde{A}_1, \dots, \tilde{A}_{N_c}] \in \mathbb{C}^{N_k \times N_c \cdot N_n}$, $\tilde{\ell} := [\tilde{l}_1, \dots, \tilde{l}_{N_c}] \in \mathbb{C}^{N_k \times N_c}$, whose columns are ordered by coils and elements' positions within the kernel (N_k, N_c, N_n are number-of-combinations/coils/neighbors). Then, the corresponding GRAPPA weights is the solution to the least squares (LS) problem,

$$\arg_{w_c} \min \|\tilde{\mathcal{A}} w_c - \tilde{l}_c\|^2 \Rightarrow w_c^\star = \tilde{\mathcal{A}}^+ \tilde{l}_c = (\tilde{\mathcal{A}}^{\mathsf{H}} \tilde{\mathcal{A}})^{-1} \tilde{\mathcal{A}}^{\mathsf{H}} \tilde{l}_c \tag{1}$$

where c indexes coils.

For arbitrary non-Cartesian readouts, where each unsampled k-space location generally has a unique pattern of sampled neighbors, it is in general not feasible to acquire the necessary ACS data for every unsampled location. Our approach is therefore to *synthesize* off-grid ACS data (for each unsampled location) from a Nyquist-sampled ACS k-space region, by using the phase-shift property of the Fourier transform (FT) (Fig.1d) such that Eq.1 can be applied (Fig.1c). This approach is general as it puts no requirement on readout trajectory, and can be fully automated, i.e., it requires no manual intervention to specify k-space wedges or other trajectory-specific information.

The main drawback of this approach is increased computational and storage costs, since for each unsampled k-space location, ACS data must be synthesized and Eq.1 must be solved. To address this computational issue, we propose a novel algorithm for obtaining the kernel weights from Eq.1. Specifically, we treat the ACS region as having circulant boundary conditions, i.e., we allow ACS data to wrap around as needed to form matches for the pattern being calibrated. When the ACS region is sufficiently large, we hypothesize that the wraparounds have negligible impact on reconstruction quality. Due to the circulant boundary, $\tilde{\mathcal{A}}_c$'s columns are circularly (phase) shifted replicas of $\tilde{l}_c$. Then, an image domain view of the solution to Eq.1 is:

$$w_c^\star = (\tilde{\mathcal{A}}^{\mathsf{H}}(\mathcal{F}\mathcal{F}^{\mathsf{H}})\tilde{\mathcal{A}})^{-1} \tilde{\mathcal{A}}^{\mathsf{H}}(\mathcal{F}\mathcal{F}^{\mathsf{H}})\tilde{l}c = (\mathcal{A}^{\mathsf{H}}\mathcal{A})^{-1}\mathcal{A}^{\mathsf{H}}l_c = ([A_1, \dots, A_{N_c}]^{\mathsf{H}}[A_1, \dots, A_{N_c}])^{-1}[A_1, \dots, A_{N_c}]^{\mathsf{H}}l_c \tag{2}$$

where unitary matrix $\mathcal{F}$ is a properly sized FT. Converted by FT, A_c's columns are (low-resolution coil images) l_c modulated by linear phases. As pointwise products of two linear phases is another a linear phase, we have (Fig.2):

$$A_i(:, m)^{\mathsf{H}} A_j(:, n) = \langle \text{diag}(\nu_m)l_i, \text{diag}(\nu_n)l_j \rangle = \langle \text{diag}(\nu_n)\nu_m, \text{diag}(l_i)l_j \rangle =: \langle \nu_{nm}, l_{ij} \rangle \tag{3}$$

where i, j are coil indices, and m,n are column indices of A_i, A_j. In other words, these entries are (spatial) frequency components of l_{ij}, which are pairwise products of low-resolution coil images (Fig.2c). The l_{ij} are shared among all kernel patterns and only need to be computed once. We propose to exploit this by first zero-padding l_i (equivalently l_{ij}), thus preparing a finely sampled spectrum. Good approximations to $\mathcal{A}^{\mathsf{H}}\mathcal{A}$ and $\mathcal{A}^{\mathsf{H}}l_c$ can then be efficiently computed (for arbitrary non-Cartesian pattern) by simple interpolations with small interpolation kernels (bilinear), instead of expensive dense matrix multiplications. This reduces computation complexity from $\Theta(N_k N_c^2 N_n^2 + N_k N_c N_n)$ to $\Theta(N_c^2 N_n^2 + N_c N_n)$, where N_k is typically a few thousand for 3D calibration (e.g., ACS size 20×20×10).

Results

Figures 3-4 compare our method with the commonly used conjugate gradient SENSE (cg-SENSE) on two 3D non-Cartesian data sets (stack-of-stars and stack-of-spirals). We reconstructed both data sets without changing the reconstruction code in any way. Different PI acceleration factors are achieved by retrospective undersampling (skipping spokes or interleaves). Our approach reconstructs images with comparable quality to cg-SENSE, using image-error

or g-factor metrics, while our approach (6secs/frame) is much faster than cg-SENSE (2mins/frame) due to its non-iterative nature. The NUFFT idea reduces calibration time from 40mins to 2mins (detailed sequence setups are described in the figure captions.)

Discussion and Conclusions:

Our results show that the proposed general, non-iterative, non-Cartesian GRAPPA algorithm can rival cg-SENSE in image quality. For reconstructing an fMRI (time-series) data set, our approach provides a fast alternative to cg-SENSE. Storage of GRAPPA kernel weights may impose high memory demands for, e.g., high-resolution imaging with a high coil count, and may benefit from coil compression.

Acknowledgements

References

1. Griswold, Mark A. et al. "Generalized Autocalibrating Partially Parallel Acquisitions (GRAPPA)." Magnetic Resonance in Medicine 47.6 (2002): 1202–1210.
2. Heidemann, Robin M. et al. "Direct Parallel Image Reconstructions for Spiral Trajectories Using GRAPPA." Magnetic Resonance in Medicine 56.2 (2006): 317–326.
3. Seiberlich, Nicole et al. "Reconstruction of Undersampled Non-Cartesian Data Sets Using Pseudo-Cartesian GRAPPA in Conjunction with GROG." Magnetic Resonance in Medicine 59.5 (2008): 1127–1137.
4. Fessler, Jeffrey A., and B.P. Sutton. "Nonuniform Fast Fourier Transforms Using Min-Max Interpolation." IEEE Transactions on Signal Processing 51.2 (2003): 560–574.

Figures
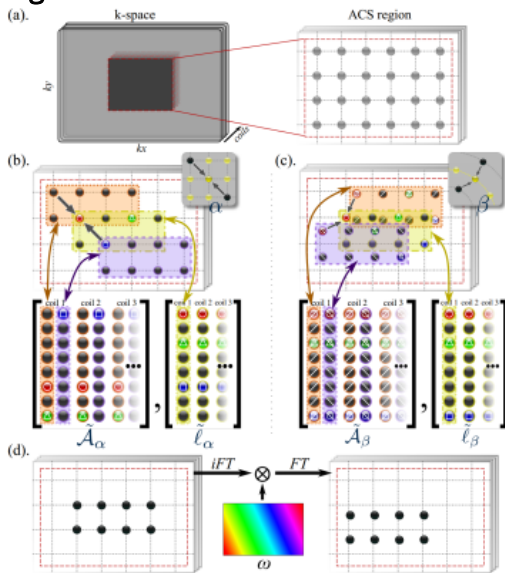
Figure 1: Constructing Cartesian and non-Cartesian GRAPPA calibration matrices. **(a)** On-grid ACS-data from dense-sampling (or gridding). **(b)** Calibration for a simple Cartesian kernel pattern α with, $N_n = 2$ neighbors used to reconstruct the center. One can obtain $N_k = 8$ combinations from the ACS region that match the relative positions described by the pattern. Neighbors and centers are separated into matrices, $\tilde{\mathcal{A}}_\alpha := [\tilde{A}_1, \ldots, \tilde{A}_{N_c}], \tilde{\ell} := [\tilde{l}_1, \ldots, \tilde{l}_{N_c}]$, where $\tilde{\mathcal{A}}_c \in \mathbb{C}^{N_k \times N_n}, \tilde{l}_c \in \mathbb{C}^{N_k}, c = 1, \ldots, N_c$. Then for coil c, least squares problem $\arg_{w_c} \min \|\tilde{\mathcal{A}} w_c - \tilde{l}_c\|^2$ gives GRAPPA weights $w_c^\star = (\tilde{\mathcal{A}}^H \tilde{\mathcal{A}})^{-1} \tilde{\mathcal{A}}^H \tilde{l}_c$. **(c)** Non-Cartesian off-grid kernel pattern β has no direct match in the on-grid ACS-data; instead, they are synthesized through phase-shifts. **(d)** Phase-shift by linear phase ω.
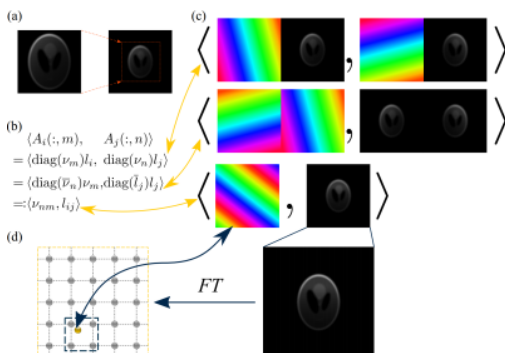
Figure 2: NUFFT-based efficient calibration algorithm using pairwise coil-image products. **(a)** Zero-padding (in image-space) of a low-resolution coil-image l_i. **(b)** Computation of an element of $\mathcal{A}^H\mathcal{A}$, which is the inner product between a column of A_i and a column of A_j. Circulant boundary makes these columns the phase-modulated low-resolution coil-images. **(c)** Visualization of (b). Linear-phases and coil-images are combined (after conjugation). **(d)** Due to the zero-padding, the spectrum is finely gridded, such that the frequency component corresponding to the combined linear phase (ν_{nm}) can be interpolated with a small kernel (bilinear) from the fixed spectrum-profile that is shared across patterns.
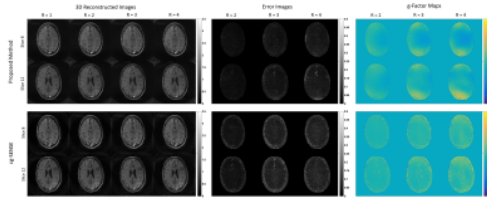
Figure 3: Stack-of-stars reconstruction results. 3D reconstruction quality comparison between the proposed non-Cartesian GRAPPA (upper row) and cg-SENSE (lower row). Panels from left to right show reconstructions with different retrospective acceleration factors (R=1,2,3,4), error images against a fully sampled reconstruction, and g-Factor maps. 2 slices are selected out of 20. Our non-Cartesian GRAPPA exhibits comparable reconstruction quality to cg-SENSE. [GE 3T scanner; 8-channel receive array; 20 kz-plates each composed of 315 spokes; FOV 20x20x20 cm^3; matrix 200x200x20; flip angle 30°; TR 15ms; minimum TE.]
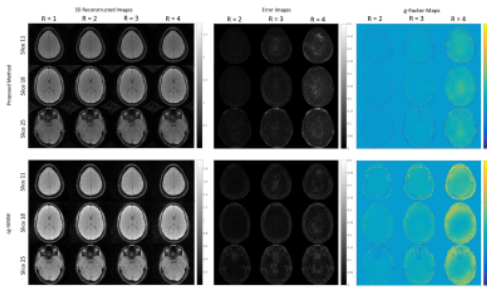
Figure 4: Stack-of-spirals reconstruction results. 3 slices are selected out of 40. Without modifying our algorithm and implementation, our non-Cartesian GRAPPA again exhibits comparable reconstruction quality to cg-SENSE. [GE 3T scanner; 8-channel receive array; 40 plates each composed of 60 spokes, FOV 22x22x20 cm^3; matrix 200x200x40, flip angle 8°, TR 15ms, minimum TE.]